Published in final edited form as:
Cancer Res. 2008 August 15; 68(16): 6831–6839. doi:10.1158/0008-5472.CAN-07-6195.

Centrosomal PKCβII and pericentrin are critical for human prostate cancer growth and angiogenesis

Jeewon Kim[1], **Yoon-La Choi**[2], **Alice Vallentin**[1], **Ben S. Hunrichs**[3], **Marc K. Hellerstein**[3,4], **Donna M. Peehl**[5], and **Daria Mochly-Rosen**[1,6]

1 *Department of Chemical and Systems Biology, Stanford University, School of Medicine, Stanford, CA, 94305*

2 *Department of Pathology, Samsung Medical Center, Sungkyunkwan University School of Medicine, Seoul, Korea*

3 *Department of Molecular and Biochemical Nutrition and Metabolism, University of California, Berkeley, CA, 94720*

4 *Department of Medicine, University of California, San Francisco, CA*

5 *Department of Urology, Stanford University, School of Medicine, Stanford, CA, 94305*

Abstract

Angiogenesis is critical in the progression of prostate cancer. However, the interplay between the proliferation kinetics of tumor endothelial cells (angiogenesis) and tumor cells has not been investigated. Also, protein kinase C (PKC) regulates various aspects of tumor cell growth but its role in prostate cancer has not been investigated in detail. Here, we found that the proliferation rates of endothelial and tumor cells oscillate asynchronously during the growth of human prostate cancer xenografts. Furthermore, our analyses suggest that PKCβII was activated during increased angiogenesis and that PKCβII plays a key role in the proliferation of endothelial cells and tumor cells in human prostate cancer; treatment with a PKCβII-selective inhibitor, βIIV5-3, reduced angiogenesis and tumor cell proliferation. We also find a unique effect of PKCβII inhibition on normalizing pericentrin (a protein regulating cytokinesis), especially in endothelial cells as well as in tumor cells. PKCβII inhibition reduced the level and mislocalization of pericentrin and normalized microtubule organization in the tumor endothelial cells. Although pericentrin has been known to be upregulated in epithelial cells of prostate cancers, its level in tumor endothelium has not been studied in detail. We found that pericentrin is upregulated in human tumor endothelium compared with endothelium adjacent to normal glands in tissues from prostate cancer patients. Our results suggest that a PKCβII inhibitor such as βIIV5-3 may be used to reduce prostate cancer growth by targeting both angiogenesis and tumor cell growth.

Introduction

In the US, prostate cancer is the third leading cause of cancer-related deaths in males (1). Although early detection and new therapies have increased survival rates, many men develop androgen-independent prostate cancers against which chemotherapeutic drugs have been generally ineffective (2). Furthermore, increases in microvessel density and expression of pro-angiogenic factors are associated with negative outcomes in patients with prostate cancer (3). Targeting cells that support tumor growth in addition to using cytotoxic agents to induce cancer cell death has therapeutic advantages (4–7). However, rather than targeting a single pro-

[6]Address for all correspondence: Daria Mochly-Rosen, Department of Chemical and Systems Biology, Stanford University, School of Medicine, Stanford, CA, 94305-5174, Tel: 650-725-7720, Fax: 650-723-4686, e-mail: mochly@stanford.edu.

angiogenic factor, there is a strong rationale for the development of new pharmacological treatments that target both tumor angiogenesis and tumor cell proliferation for the treatment of prostate cancer (8).

The protein kinase C (PKC) family of serine/threonine kinases plays an important role in angiogenesis both *in vitro* and *in vivo* (9–12). Also, PKC is activated by tumor-promoting phorbol esters and its involvement in carcinogenesis was proposed many years ago (13). Its role has since been substantiated in many human cancers, including prostate cancer (14–17). However, the role of PKC in prostate cancer angiogenesis has not been explored explicitly. Currently, a PKCβ inhibitor, Enzastaurine (a novel macrocyclic bisindolylmaleimide), is being tested in clinical trials for its anti-angiogenic and anti-cancer effects with promising phase II studies of high-grade gliomal tumors (18). However, although the initial reports suggested that Enzastaurine is selective for PKCβ (15), subsequent studies showed that it also inhibits PKCγ, δ, and ε to a similar degree at the same concentration (14).

PKC family members are known to mediate cytokinesis and cell proliferation by microtubule regulation (19-21). Functional studies have shown a key role for pericentrin, a centrosomal protein, in microtubule organization, spindle assembly, and chromosome segregation (22,23). Chen et al. showed that endogenous PKCβII and pericentrin interact in K562 cells (19) and that PKCβII co-localizes with pericentrin in G_2 and mitotic cells, i.e. dividing cells in culture. In addition, overexpression of a fragment of pericentrin that binds PKCβII leads to mislocalization of PKCβII away from the centrosome and a loss of microtubule anchoring at the centrosome resulting in cytokinesis failure and aneuploidy. Also, overexpression of a PKCβII fragment that binds pericentrin induces the same phenotype, suggesting that increased levels of PKCβII could also disrupt interaction with pericentrin. Therefore, there is strong evidence that PKCβII and pericentrin regulate cytokinesis in cells, but the role of PKCβII and pericentrin in prostate cancer progression, both in endothelial and tumor cells *in vivo*, has not been established.

Here, we set out to determine how PKC activity affects angiogenesis and tumor cell proliferation during different stages of prostate tumor growth in a xenograft model. Our data from xenografts and patients suggest PKCβII as a target in anti-cancer treatment for prostate cancer against tumor-induced angiogenesis and tumor growth.

Materials and Methods

Cell lines and cell culture

PC-3 human prostate cancer cells and mouse tumor endothelial cells (2H-11) were obtained from the American Type Culture Collection (ATCC, Manassas,VA) and cultured in DMEM media with 10% fetal bovine serum (FBS, Gibco, NY) with 1% antibiotics (penicillin and streptomycin, Gibco, NY). Primary cultures of normal human epithelial cells were established from the peripheral zone of a radical prostatectomy specimen according to established techniques (24). The tissue of origin was confirmed to be normal by histopathological analyses. Cells were cultured in a serum-free medium, “Complete PFMR-4A” (24). For *in vitro* tumor endothelial cell culture, 5000 cells were seeded into each well of chamber slides in DMEM with 10% FBS and grown for 2 days in DMEM or conditioned medium from PC-3, i.e. 2 day old medium from PC-3 cell cultures. Tumor endothelial cells were then treated with TAT (carrier peptide) or βIIV5-3-TAT at a final concentration of 1 μM, 3 times per day for 2 days.

Materials

For Western blot analyses, rabbit antibodies directed against Gαi-3 (C-10) were from Santa Cruz Biotechnology, Inc. (Santa Cruz, CA) and anti-GAPDH antibody, clone 6C5, was from

Advanced Immunochemical (Long Beach, CA). For immunofluorescence, α-tubulin and γ-tubulin Cy3 antibodies were from Sigma (St. Louis, MO). Pericentrin antibodies used for immunofluorescence were from Abcam (4448, Cambridge, MA). Pericentrin antibodies used for Western blot analyses (M1, 4b and UM225) were from Dr. Stephen Doxsey (University of Massachusetts, Worcester, MA). Paraffin-embedded prostate tissues were from the Urology Department at Stanford Medical School (IRB # 348).

Peptide synthesis and administration

The PKCβII-selective inhibitor (βIIV5-3) was derived from the PKCβII V5 region (amino acids 645–650 [QEVIRN]) (25). For intracellular delivery, peptides were synthesized and conjugated to a membrane-permeable TAT carrier peptide as previously described (26). TAT carrier peptide or saline was used as a control. Peptides were delivered *in vivo* using Alzet osmotic mini-pumps (Alzet model 2001) as described (27). The peptides were dissolved in saline and administered at a constant rate (0.5μl/hr) corresponding to 2.4 or 24 mg/day/kg (3mM or 30mM of TAT) and 3.6 or 36 mg/day/kg (3mM or 30mM of βIIV5-3-TAT). Pumps were replaced every 2 weeks because of the $t_{1/2}$ (about 2 weeks) of the peptides in the pump (27). Peptides were delivered for up to 5 weeks.

Xenograft tumor studies

Six week old male nude mice were purchased from Harlan (Indianapolis, IN) and housed at the animal care facility at Stanford University Medical Center (Stanford, CA). All mice were kept under standard temperature, humidity, and timed lighting conditions and provided mouse chow and water *ad libitum.* All animal experimentation was conducted in accordance with the Guide for Care and Use of Laboratory Animals prepared by the Institute of Laboratory Animal Resources, National Research Council, and published by the National Academy Press (revised 1996) and was approved by the Stanford University Animal Care and Use Committee. Five million PC-3 tumor cells were injected subcutaneously in the flank of male, 7–8 week old, athymic nude mice in sterile PBS (Figure 2) or in a mixture of 1:1 serum-free medium and Matrigel (Figure 3, Beckton Dickinson, Bedford, MA). Peptide treatment began when the tumors reached a group average of 100mm^3 after about 1 week. Tumor volume (mm^3) was calculated using the equation $0.52\times (\text{width (cm)})^2 \times (\text{length (cm)})$.

Measurement of cell proliferation

Animals were administered 4% deuterated water and tumor endothelial cells and tumor cells were isolated using flow cytometric sorting (refer to supplemental Figure 1 for cell isolation) and prepared for GC-MS analyses as previously described (28, 29).

Immunofluorescence

Dual-color immunofluorescence was performed on fresh-frozen sections fixed in O.T.C. compound (Torrance, CA) using PKC and biotin linked rat-anti mouse CD31 antibodies (Santa Cruz Biotech Inc, Santa Cruz, CA and BD Pharmingen, San Diego, CA, respectively). For pericentrin and PKC detection, sections were stained with rabbit anti-pericentrin (ab4448, Abcam, Cambridge, MA) followed by PKC antibodies. TUNEL staining was carried out using an *in situ* cell death detection kit (TMR red) according to manufacturer's instructions (Roche Applied Science, Indianapolis, IN). Cleaved caspase-3 antibody was from Cell Signaling (Danvers, MA). CD31- and TUNEL-positive areas were measured using Photoshop (Version 9.0.1). Hoechst 333242 was from Molecular Probes (Carlsbad, CA). The apparatus for immunofluorescence experiments consisted of a Leica DMI 6000B microscope with 350FX camera (JH Technologies, San Jose, CA).

Immunoblot analysis

Frozen tumors and livers were weighed and two volumes of homogenization buffer [20 mM Tris-HCl, pH 7.5, 2 mM EDTA, 10 mM EGTA, 250 mM sucrose, 1:300 protease inhibitor cocktail (Sigma) and 1:300 phosphatase inhibitor cocktail (Sigma)] were added. The tissue was homogenized and were fractionated by spinning at 100,000g for 30 min at 4°C. The supernatants correspond to the cytosolic fractions. The particulate fractions correspond to the rest of the intracellular organelles including nuclear and plasma membrane. The particulates were resuspended in homogenization buffer with 1% Triton X-100 and both detergent soluble and insoluble fractions were analyzed together. Translocation of PKCα, βI, βII and ε was determined in cytosolic and particulate fractions from tumor and liver samples as described (26). Whole cell lysates refer to total homogenates without fractionation. For all PKC detections, 10 μg of whole cell lysates, cytosolic and particulate fractions were used. Antibodies against GAPDH (1:10,000) and Gαi-3 (1:1000) were used as loading controls for cytosolic and particulate fraction, respectively.

Kinase assay after immunoprecipitation

Tumor lysates were subjected for immunoprecipitation using PKCβ II according to Chen et al. (19) and the immunoprecipitate was assayed for kinase activity in the absence of PKC activators (30).

Immunohistochemistry

Tissue sections in the slides were deparaffinized and with xylene, hydrated by using a diluted alcohol series, and immersed in 3% H_2O_2 in distilled water for 15 minutes to quench endogenous peroxidase activity. The sections were then microwaved in a pressure cooker for 30 minutes in distilled water containing 1mM EDTA. To avoid non-specific staining, each section was incubated with 4% bovine serum albumin (Qbiogene, Irvine, CA) in PBS with 0.1% Tween 20 (PBST) for 30 minutes at room temperature. The sections were then incubated with rabbit anti-pericentrin polyclonal antibody (4b, dilution: 1:250) in TBST [50mM Tris (pH7.5), 150mM NaCl, and 0.5% Tween 20] containing 4% Tryptone casein (Amresco, Solon, OH) for 1 hour at room temperature. HRP-conjugated secondary antibody against rabbit immunoglobulins (DAKO, Carpinteria, CA) was applied for 20 min at room temperature. Signals were amplified by catalyzed reporter deposition tyramine signal amplification (CSA II kit, DAKO, Carpinteria, CA), following manufacturer's instructions. Each section was incubated with fluorescyl-conjugated tyramide for 15 minutes and protected from light. Sections were then incubated with HRP-conjugated anti-fluorescein antibody for 15 minutes at room temperature. Each step was followed by three successive rinses with TBST for 5 min. The chromogen used was 3,3′-diaminobenzidine (DAKO, Carpinteria, CA). Sections were counterstained in Meyer's hematoxylin.

Statistical analysis

Data are expressed as mean±SE. Paired *t* test and repeated ANOVA were used to assess significance ($p<0.05$).

Results

High levels of PKCβII are present in growing tumors and in the tumor endothelium

Because PKC activation has been implicated during growth of various tumors (31,32), we first determined which PKC isozyme is present in growing PC-3 human prostate cancer cells in a xenograft model, *in vivo*. PKCα, βI, βII and ε were all found in the PC-3 tumors (Figure 1A). We next compared the cellular distribution of the PKC isozymes in the PC-3 xenografts with that in a primary culture of normal human prostate epithelial cells (PEC). We used the cellular

distribution of the isozymes in PEC as a measure of basal levels of PKC activation (Figure 1A, left; cytosolic enzyme represents inactive PKC (33)). All the PKC isozymes were more active in the PC-3 xenografts relative to the primary PEC and PKCβII appeared more active relative to the other isozymes, as evidenced by high levels of this isozyme in the particulate fraction relative to the cytosolic fraction. This was also apparent when comparing PKCβII and its alternatively spliced form, PKCβI (n=4 each, p=0.01, Figure 1A, right). Immunofluorescence studies demonstrated that PKCβII was more localized to endothelial cells relative to PKCα, βI or ε (Figure 1B, arrow heads). Based on these results, we focused our study on determining the role of PKCβII in angiogenesis and in tumor growth.

Increase in proliferation rate of tumor endothelial cells precedes that of tumor cells

To examine the proliferation kinetics of tumor cells and endothelial cells in the growing tumor, we used a new method that measures directly the proliferation rates of these cells, *in vivo* (Figure 2A, B, C). PC-3 cancer cells were injected subcutaneously (5×10^6 cells) into the flank area of male nude mice and the resulting solid tumors were isolated each week, for up to 6 weeks after tumor cell injection (Figure 2A, B). For each time point, deuterated water was administered in drinking water for 1 week before sacrificing and the tumor endothelial cells and tumor cells were isolated by fluorescence activated cell sorting (FACS). The proliferation rate of each cell type was calculated by measuring the amount of deuterium in the DNA of these cells, as we previously described (28, 29).

Interestingly, the rise in tumor endothelial cell (TEC) proliferation rate preceded the rise in the proliferation rate of the tumor cells (TC) during the first 4 weeks (Figure 2C); rates of proliferation of these two cell types continued to change in an oscillating pattern for about 4 weeks. These data support the predicted coordination between tumor growth and angiogenesis with TEC proliferation and angiogenesis rising to meet the metabolic demand of the growing tumor (4, 34). After week 4, the tumor endothelial cell and tumor cell proliferation rates appeared to reach a steady-state, suggesting that the rate of angiogenesis had matched the metabolic demand of the growing tumor (4, 34). We further examined the kinetics of cell proliferation during the days 0–7 of post-tumor injection (n=6–10 animals each, insert). The proliferation rate of tumor endothelial cells was several-fold higher than that of tumor cells during days 0–4 and days 4–7 (Figure 2C, insert), indicating active tumor angiogenesis during the early period of tumor growth with only moderate tumor cell proliferation at that period. This confirms that angiogenesis is particularly active in the early period of tumor growth and suggests a window of treatment for anti-angiogenesis.

A PKCβII-specific inhibitor effectively reduced PC-3 tumor growth rate

Because we found PKCβII to localize mainly in endothelial cells, we next determined its role in tumor growth and angiogenesis, *in vivo*. We implanted osmotic pumps with saline, control peptide ($TAT_{47–57}$ carrier peptide (35,36)) or βIIV5-3 (PKCβII-selective inhibitor peptide) conjugated to $TAT_{47–57}$ to deliver the PKCβII inhibitor (25) into the cells. Specifically, one week after injection of the PC-3 cells, mice were implanted with osmotic pumps with saline/TAT or βIIV5-3 at 3.6 mg/kg/day for 2 weeks followed by 36 mg/kg/day for the following 3 weeks. Already after two weeks of treatment, there was a trend towards decreased tumor size in the βIIV5-3-treated animals (Figure 3A). When the βIIV5-3 concentration was increased from 3.6 mg/kg/day to 36 mg/kg/day for the next 3 weeks [a dose that was well tolerated (37)], tumor volume was found to be significantly smaller in the βIIV5-3-treated group over time (Figure 3A, repeated ANOVA, *; $p<0.05$, n=4–5 each). Previous *in vivo* studies demonstrated that inhibition of PKC translocation by systemic peptide delivery was observed in all tissues (26). Similarly, we found here that βIIV5-3 treatment reduced the level of PKCβII in the particulate fraction relative to the cytosolic fraction in tumor as well as in other tissues *e.g.*, in liver (βIIV5-3 treatment decreased PKCβII translocation by 25–35%; Figure

3B, right, $p<0.05$, n=3 each). We have previously shown that such a decrease in PKC translocation is sufficient to inhibit its pathological activity [*e.g*., (38,39)]. We further confirmed the selectively of the PKCβII inhibitor; sustained treatment of βIIV5-3 did not affect translocation of the closely related PKCμI in the tumor nor PKCε in the liver (supplemental Figure 3). Using kinase assay *in vitro* in the absence of added PKC activators, we found that βIIV5-3 treatment resulted in an ~85% reduction in the catalytic activity of PKCβII immunoprecipitated from total tumor lysates containing equal amounts of protein (Figure 3C), confirming sustained inhibition of PKCβII in the treated tumors.

We next set out to confirm the tumor growth inhibitory effect *in vivo* by administering βIIV5-3 at the higher dose of 36 mg/kg/day from week 1 - week 5 (*i.e.*, when we observed the most active angiogenesis, see Figure 2C). This treatment decreased overall tumor growth rate by 60% compared to 16% with the lower dose of βIIV5-3, calculated as the change in tumor volume over time (Figure 3D; $p<0.05$, n=8–9 each *vs.* Figure 3A).

βIIV5-3 decreased proliferation rates of tumor endothelial cells and tumor cells

Next, we determined whether βIIV5-3 affected cell division of tumor endothelial cells by directly measuring *in vivo* cell proliferation rates using deuterated water, as in Figure 2. At week 3 with two weeks of sustained treatment with βIIV5-3 (3.6 mg/kg/day), tumor endothelial cell (TEC) proliferation rates were reduced by 40%, as compared to control mice (Figure 4A, $p=0.008$, n=8–9 each). However, there was no difference in the proliferation rates five weeks after sustained treatment (at week 6) of βIIV5-3 (3.6 mg/kg/day followed by 36 mg/kg/day). These data suggest that the anti-angiogenic effect of β IIV5-3 is more pronounced at the early stage of tumor growth, even at a lower dose. To confirm the anti-angiogenic effect of βIIV5-3, tumor sections at week 3 and 6 were stained with anti-CD31 antibody, a marker of endothelial cells (Figure 4B). There was a significantly lower number of CD31-positive tumor vessels in the βIIV5-3-treated samples compared to controls at week 3 (28±11 *vs*. 6±3 %, $p<0.05$, Figure 4B), but not at week 6 (not significant, data not shown), quantified using Photoshop program (Ver. 9.0.1, San Jose, CA).

βIIV5-3 treatment also decreased tumor cell (TC) proliferation rates at week 3 (Figure 4C, $p<0.001$) and showed a trend for inhibition at week 6 ($p=0.065$, Figure 4C). Moreover, there was a stronger tendency of increased TUNEL-positive cells in the βIIV5-3-treated tumors at week 6 relative to TAT or saline controls (Figure 4D, 2±1 *vs*. 8±2 %, p=0.06), compared to week 3 (not significant). We found that TUNEL-positive cells overlapped with staining for cleaved caspase 3 (Figure 4D, insert), further confirming an increase in apoptosis. This suggests that at an earlier tumor stage, βIIV5-3 treatment decreases cell proliferation of both the tumor endothelial cells and tumor cells rather than inducing apoptosis.

βIIV5-3 treatment induced co-localization of PKCβII and pericentrin in PC-3 tumors

We next set out to determine the molecular basis for inhibition of tumor growth by β IIV5-3. An unbiased two hybrid screen by Newton and collaborators demonstrated that a centrosomal protein, pericentrin, which is involved in controlling cytokinesis, microtubule organization and spindle formation, binds PKCβII (19).

Pericentrin levels in human prostate cancer have been shown to be elevated with increasing Gleason grade (23,40). Furthermore, pericentrin overexpression is associated with centrosomal defects leading to chromosomal instability, microtubule mis-segregation, larger nuclei and increased cell proliferation in human prostate and other types of cancer cells (23,40–43). We therefore hypothesized that regulation of interaction of PKCβ II with pericentrin may play a role in the phenotype that we observed. Pericentrin staining appears as a dot or two in normal cells (19,23,40 and in supplemental Figure 2). However, staining of the PC-3 tumor xenografts

showed an abnormal pattern of pericentrin staining with elongated filamentous structures (Figure 5A, left panel). Treatment with 36 mg/kg/day of βIIV5-3 for 4 weeks significantly reduced the abnormal filamentous pericentrin staining, reduced the overall staining intensity and resulted in the return of a dotted staining pattern with anti-pericentrin antibodies (Figure 5A, right panel). This was confirmed by Western blot analyses of pericentrin (~220kDa) and its cleaved form (~150kDa) in the total tumor lysate (Figure 5B). The amount of cleaved form of pericentrin was reduced by ~90% with βIIV5-3 treatment compared to TAT controls (Figure 5B, lower arrow). We also found that enlongated and filamentous pericentrin did not co-localize with PKCβII in TAT-treated tumors (asterisk, Figure 5C,2,3,4), whereas dotted pericentrin co-localized with PKCβII in βIIV5-3-treated tumors (arrows, Figure 5C,6, 7, 8). This was confirmed by determining the interaction between pericentrin and PKCβII *in vivo* by co-immunoprecipitation assay followed by Western blot analysis of the immunoprecipitate. PKCβII was immunoprecipitated from the total tumor lysate using anti-PKCβII antibodies and detected with antibodies against pericentrin (Figure 5D, upper panel, lanes 2 and 3). We detected pericentrin (~220kDa) and its cleaved form (~150kDa) in the immunoprecipitate (44,45). Even though the total level of pericentrin was lower in the βIIV5-3-treated group as compared with the TAT-treated group (Figure 5B), there was 10-fold more pericentrin associated with PKCβII as compared with that associated in immunoprecipitates from TAT-treated tumors (Figure 5D, upper panel, lanes 2 and 3). Immunoprecipitate from the lysate of primary culture of PECs that were not treated with βIIV5-3 was also used to show interaction of PKCβII and pericentrin in normal human cells. The interaction between PKCβII and pericentrin was stronger than that in untreated PC-3 tumors (Lane 5).

Abnormal pericentrin staining in the tumor endothelial cells and in human tumor endothelium

Because we found that filamentous pericentrin was present in structures similar to microvessels (Figure 5A, left panel), we co-stained tumor sections for CD31 (a marker of vessels) and pericentrin. In TAT-treated tumors, enlongated and filamentous pericentrin was seen in tumor vessels (Figure 6A, left panel, arrows). In βIIV5-3-treated tumors, pericentrin staining was significantly reduced in tumor microvessels and dotted staining was apparent in both tumor cells (arrow heads) and tumor endothelium (arrows, Figure 6A, right panel).

Since tumor endothelial cells are contributed by the mice, we used a mouse tumor endothelial cell line cultured in medium from PC-3 human cancer cells to simulate *in vivo* system (46). Medium from PC-3 cells increased the level of pericentrin staining in the endothelial cells (Figure 6B, left panel, middle row) relative to those cultured in normal DMEM (Figure 6B, left panel, top row). βIIV5-3 treatment reduced this effect (Figure 6B, left panel, bottom row). To confirm that the pericentrin abnormality correlates with centrosomal defect, endothelial cells were also stained for γ-tubulin (Figure 6B, middle panel). PC-3-conditioned medium increased the centrosomal γ-tubulin staining in the endothelial cells (Figure 6B, second panel, middle row) whereas βIIV5-3 treatment normalized it similarly to TAT-treated cells (Figure 6B, second panel, bottom and top rows). Also, PC-3-conditioned medium resulted in disorganized forms of α-tubulin, representative of microtubule organization (Fig. 6C, second panel, middle row) in the endothelial cells, whereas βIIV5-3 treatment resulted in an organized form of microtubules, similar to TAT - treated cells in DMEM (Fig. 6C, second column, bottom and top rows).

To determine the clinical relevance of our findings, we assessed location and levels of pericentrin in prostate tissue from patients with Gleason grades 3, 4 and 5 cancers. Similar to our data in the xenograft model, in some patients, we found higher levels of pericentrin in the cytoplasm of endothelial cells adjacent to tumor glands (Figure 6D, middle, 100X) compared to those among benign prostatic hyperplasia (Figure 6D, left, 100X). The figure on the right is

showing a magnified view of the middle figure (right, 400X). In tumors of other patients, some tumor endothelial cells were strongly stained for pericentrin, whereas others were stained at similar levels to those seen in endothelial cells among normal glands. These data suggest that, at least in some patients with Gleason grades 3 and up prostate cancers, there is upregulation of pericentrin levels and localization in tumor endothelium.

Discussion

Determining isozyme-specific roles of PKC in tumors has been hampered by a lack of `isozyme-specific regulators for each PKC isozyme. Here, we show that isozyme-specific inhibition of PKCβII by βIIV5-3 reduces PC-3 tumor growth in a xenograft model by decreasing angiogenesis, tumor cell proliferation and normalizing pericentrin levels and subcellular localization.

First, we found an oscillatory pattern of increase in the proliferation rates of tumor endothelial and tumor cells. This *in vivo* interplay between the tumor endothelial cells and tumor cell proliferation has not been reported and provides a new insight into the relationship between the tumor and microenvironment during prostate cancer progression. These findings also identified a possible time window for drug treatment to reduce angiogenesis and tumor growth. Our findings may relate to the alternate apoptotic waves of these two cells types in Lewis lung carcinoma xenografts with chemotherapy as evidenced by TUNEL staining (6,34); both are likely reflecting the tight regulation of angiogenesis by the tumor, to match metabolic demand of the tumor mass.

Microvessel density, the most frequently used method to measure angiogenesis, is not without limitations (4); vessel density does not represent the angiogenic activity of the tumor. Rather, it represents local tumor metabolic burden expressed as vessel to tumor ratio (4). Also, this measurement is laborious and quite subjective (47). We therefore used $^{2}H_2O$ to label DNA *in vivo*. Our method accurately measures net *in vivo* proliferation (*i.e.* turnover) rates of the tumor cells and the endothelial cells separately during the $^{2}H_2O$ administration period (28,29) by analyzing isolated endothelial cells and tumor cells from the tissue (see supplemental Figure 1).

PKC family members are known to mediate cytokinesis and cell proliferation by regulation of microtubule organization (19–21). Expression studies of pericentrin fragments in cultured cells demonstrated a key role for pericentrin as a scaffold protein for PKCβII in microtubule organization, spindle assembly, and chromosome segregation (19). Here, βIIV5-3 appeared to normalize centrosome defects and microtubule misalignment seen in tumor endothelial cells. Knockdown of pericentrin in TEC and PC-3 cells using siRNA resulted in decreased γ-tubulin staining and reduction in the number of cells, supporting our data (supplemental Figure 4B and C). Because centrosome aberration and microtubule misorganization are thought to be possible causes of aneuploidy and chromosomal instability in some types of cancer, including prostate cancer (40,41), the role of PKCβII/pericentrin interaction in the molecular events leading to aberration in cytokinesis and chromosomal mis-segregation needs to be determined. The cleaved form of pericentrin was suggested to be involved in malignant transformation (44, 45). Increased binding of PKCβII to pericentrin, especially the cleaved form, may inhibit further carcinogenesis. The effect of βIIV5-3, which inhibits the binding of PKCβII to its RACK, a receptor for activated C kinase (25,48), may leave more PKCβII available for binding with pericentrin at the centrosome. We also found increased staining of pericentrin in endothelial cells can be induced by PKCβII-activating factor(s) secreted from the tumor cells. Our data suggest that the secreted factor is unlikely to be VEGF (see supplemental Figure 5); the role of other secreted factors from prostate cancer cells (*e.g.* TGF-α, basic fibroblast growth factor and insulin-like growth factor (3)) remains to be determined.

The findings that pericentrin levels are greatly elevated in human prostate tumors relative to normal prostate tissue, that pericentrin levels correlate with the Gleason grade (23,40) and our immunohistochemistry data of high levels of pericentrin, specifically in the tumor endothelium (Figure 6D) of some patients suggest that correction of pericentrin abnormalities with a PKCβII inhibitor, such as βIIV5-3, may improve both anti-angiogenic and anti-tumor therapy. It remains to be determined whether the catalytic activity of PKCβII plays a role in pericentrin regulation or whether its role is confined to simply anchoring pericentrin. Our data also suggest that a larger study of humans with prostate cancer is warranted, to assess the correlation between the levels of pericentrin in tumor endothelium and the Gleason grade of the cancer.

In conclusion, we show that an isozyme-specific inhibitor of PKCβII localization and function reduces tumor growth by reducing angiogenesis and tumor cell proliferation in a human prostate cancer xenograft model. We determined the appropriate window of treatment by analyzing proliferation kinetics of tumor endothelial cells and tumor cells *in vivo* using a direct measurement of cell proliferation. PKCβII inhibition corrected pericentrin localization and reduced other abnormalities, especially in the tumor vessels. Overall, our results suggest that a PKCβII inhibitor may provide a useful adjuvant treatment to the current therapy for patients with prostate cancer (and perhaps for patients with other solid tumors) by inhibiting proliferation of both tumor endothelial cells as well as tumor cells in the early phase.

Supplementary Material

Refer to Web version on PubMed Central for supplementary material.

Acknowledgements

This study was supported in part by PHS Grant Number CA09151 awarded by the National Cancer Institute, DHHS to J Kim.

DMR is the founder of KAI Pharmaceuticals, Inc., a company that plans to bring PKC regulators to the clinic. However, none of the work described in this study is based on or is supported by the company.

References

1. Nelson WG. Prostate cancer prevention. Curr Opin Urology 2007;17:157–67.
2. Walczak JR, Carducci MA. Prostate cancer: a practical approach to current management of recurrent disease. Mayo Clin Proc 2007;82:243–9. [PubMed: 17290734]
3. Charlesworth PJ, Harris AL. Mechanisms of disease: angiogenesis in urologic malignancies. Nat Clin Pract Urol 2006;3:157–69. [PubMed: 16528288]
4. Hlatky L, Hahnfeldt P, Folkman J. Clinical application of antiangiogenic therapy: microvessel density, what it does and doesn't tell us. J Natl Cancer Inst 2002;94:883–93. [PubMed: 12072542]
5. Folkman J. The role of angiogenesis in tumor growth. Semin Cancer Biol 1992;3:65–71. [PubMed: 1378311]
6. Browder T, Butterfield CE, Kraling BM, et al. Antiangiogenic scheduling of chemotherapy improves efficacy against experimental drug-resistant cancer. Cancer Res 2000;60:1878–86. [PubMed: 10766175]
7. Burdelya LG, Komarova EA, Hill JE, et al. Inhibition of p53 Response in Tumor Stroma Improves Efficacy of Anticancer Treatment by Increasing Antiangiogenic Effects of Chemotherapy and Radiotherapy in Mice. Cancer Res 2006;66:9356–61. [PubMed: 17018587]
8. Faivre S, Djelloul S, Raymond E. New paradigms in anticancer therapy: targeting multiple signaling pathways with kinase inhibitors. Semin Oncol 2006;33:407–20. [PubMed: 16890796]
9. Griner EM, Kazanietz MG. Protein kinase C and other diacylglycerol effectors in cancer. Nat Rev Cancer 2007;7:281–94. [PubMed: 17384583]

10. Das Evcimen N, King GL. The role of protein kinase C activation and the vascular complications of diabetes. Pharmacol Res 2007;55:498–510. [PubMed: 17574431]
11. Montesano R, Orci L. Tumor-promoting phorbol esters induce angiogenesis in vitro. Cell 1985;42:469–77. [PubMed: 2411423]
12. Takahashi T, Ueno H, Shibuya M. VEGF activates protein kinase C-dependent, but Ras-independent Raf-MEK-MAP kinase pathway for DNA synthesis in primary endothelial cells. Oncogene 1999;18:2221–30. [PubMed: 10327068]
13. Castagna M, Takai Y, Kaibuchi K, Sano K, Kikkawa U, Nishizuka Y. Direct activation of calcium-activated, phospholipid-dependent protein kinase by tumor-promoting phorbol esters. J Biol Chem 1982;257:7847–51. [PubMed: 7085651]
14. Graff JR, McNulty AM, Hanna KR, et al. The protein kinase Cbeta-selective inhibitor, Enzastaurin (LY317615.HCl), suppresses signaling through the AKT pathway, induces apoptosis, and suppresses growth of human colon cancer and glioblastoma xenografts. Cancer Res 2005;65:7462–9. [PubMed: 16103100]
15. Teicher BA, Alvarez E, Menon K, et al. Antiangiogenic effects of a protein kinase Cbeta-selective small molecule. Cancer Chemother Pharmacol 2002;49:69–77. [PubMed: 11855754]
16. Teicher BA, Menon K, Alvarez E, Shih C, Faul MM. Antiangiogenic and antitumor effects of a protein kinase Cbeta inhibitor in human breast cancer and ovarian cancer xenografts. Invest New Drugs 2002;20:241–51. [PubMed: 12201487]
17. Koren R, Ben Meir D, Langzam L, et al. Expression of protein kinase C isoenzymes in benign hyperplasia and carcinoma of prostate. Oncol Rep 2004;11:321–6. [PubMed: 14719062]
18. Green LJ, Marder P, Ray C, et al. Development and validation of a drug activity biomarker that shows target inhibition in cancer patients receiving enzastaurin, a novel protein kinase C-beta inhibitor. Clin Cancer Res 2006;12:3408–15. [PubMed: 16740765]
19. Chen D, Purohit A, Halilovic E, Doxsey SJ, Newton AC. Centrosomal anchoring of protein kinase C betaII by pericentrin controls microtubule organization, spindle function, and cytokinesis. J Biol Chem 2004;279:4829–39. [PubMed: 14594954]
20. Kiley SC, Parker PJ. Differential localization of protein kinase C isozymes in U937 cells: evidence for distinct isozyme functions during monocyte differentiation. J Cell Sci 1995;108(Pt 3):1003–16. [PubMed: 7622590]
21. Takahashi M, Mukai H, Oishi K, Isagawa T, Ono Y. Association of immature hypophosphorylated protein kinase cepsilon with an anchoring protein CG-NAP. J Biol Chem 2000;275:34592–6. [PubMed: 10945988]
22. Doxsey SJ, Stein P, Evans L, Calarco PD, Kirschner M. Pericentrin, a highly conserved centrosome protein involved in microtubule organization. Cell 1994;76:639–50. [PubMed: 8124707]
23. Pihan GA, Purohit A, Wallace J, Malhotra R, Liotta L, Doxsey SJ. Centrosome defects can account for cellular and genetic changes that characterize prostate.
24. Peehl, DM. Human prostatic epithelial cells. In: Freshney, RI.; Freshney, MG., editors. Culture of Epithelial Cells. New York: Wiley-Liss; 2002. p. 171-94.
25. Stebbins EG, Mochly-Rosen D. Binding specificity for RACK1 resides in the V5 region of beta II protein kinase C. J Biol Chem 2001;276:29644–50. [PubMed: 11387319]
26. Begley R, Liron T, Baryza J, Mochly-Rosen D. Biodistribution of intracellularly acting peptides conjugated reversibly to Tat. Biochem Biophys Res Commun 2004;318:949–54. [PubMed: 15147964]
27. Inagaki K, Begley R, Ikeno F, Mochly-Rosen D. Cardioprotection by epsilon-protein kinase C activation from ischemia: continuous delivery and antiarrhythmic effect of an epsilon-protein kinase C-activating peptide. Circulation 2005;111:44–50. [PubMed: 15611364]
28. Kim SJ, Cheung S, Hellerstein MK. Isolation of nuclei from label-retaining cells and measurement of their turnover rates in rat colon. Am J Physiol Cell Physiol 2004;286:C1464–73. [PubMed: 14960413]
29. Neese RA, Misell LM, Turner S, et al. Measurement in vivo of proliferation rates of slow turnover cells by 2H2O labeling of the deoxyribose moiety of DNA. Proc Natl Acad Sci U S A 2002;99:15345–50. [PubMed: 12424339]

30. Disatnik MH, Boutet SC, Lee CH, Mochly-Rosen D, Rando TA. Sequential activation of individual PKC isozymes in integrin-mediated muscle cell spreading: a role for MARCKS in an integrin signaling pathway. J Cell Sci 2002;115:2151–63. [PubMed: 11973356]

31. Hofmann J. Protein kinase C isozymes as potential targets for anticancer therapy. Curr Cancer Drug Targets 2004;4:125–46. [PubMed: 15032665]

32. Koivunen J, Aaltonen V, Peltonen J. Protein kinase C (PKC) family in cancer progression. Cancer Lett 2006;235:1–10. [PubMed: 15907369]

33. Kraft AS, Anderson WB, Cooper HL, Sando JJ. Decrease in cytosolic calcium/phospholipid-dependent protein kinase activity following phorbol ester treatment of EL4 thymoma cells. J Biol Chem 1982;257:13193–6. [PubMed: 7142138]

34. Folkman J. Angiogenesis and apoptosis. Semin Cancer Biol 2003;13:159–67. [PubMed: 12654259]

35. Chen L, Wright LR, Chen CH, Oliver SF, Wender PA, Mochly-Rosen D. Molecular transporters for peptides: delivery of a cardioprotective epsilonPKC agonist peptide into cells and intact ischemic heart using a transport system, R(7). Chem Biol 2001;8:1123–9. [PubMed: 11755391]

36. Schwarze SR, Ho A, Vocero-Akbani A, Dowdy SF. In vivo protein transduction: delivery of a biologically active protein into the mouse. Science 1999;285:1569–72. [PubMed: 10477521]

37. Koyanagi T, Noguchi K, Ootani A, Inagaki K, Robbins RC, Mochly-Rosen D. Pharmacological inhibition of epsilon PKC suppresses chronic inflammation in murine cardiac transplantation model. J Mol Cell Cardiol 2007;43:517–22. [PubMed: 17655859]

38. Bright R, Raval AP, Dembner JM, et al. Protein kinase C delta mediates cerebral reperfusion injury in vivo. J Neurosci 2004;24:6880–8. [PubMed: 15295022]

39. Murriel CL, Churchill E, Inagaki K, Szweda LI, Mochly-Rosen D. Protein kinase Cdelta activation induces apoptosis in response to cardiac ischemia and reperfusion damage: a mechanism involving BAD and the mitochondria. J Biol Chem 2004;279:47985–91. [PubMed: 15339931]

40. Pihan GA, Wallace J, Zhou Y, Doxsey SJ. Centrosome abnormalities and chromosome instability occur together in pre-invasive carcinomas. Cancer Res 2003;63:1398–404. [PubMed: 12649205]

41. Nakajima T, Moriguchi M, Mitsumoto Y, et al. Centrosome aberration accompanied with p53 mutation can induce genetic instability in hepatocellular carcinoma. Mod Pathol 2004;17:722–7. [PubMed: 15044920]

42. Neben K, Tews B, Wrobel G, et al. Gene expression patterns in acute myeloid leukemia correlate with centrosome aberrations and numerical chromosome changes. Oncogene 2004;23:2379–84. [PubMed: 14767474]

43. Schneeweiss A, Sinn HP, Ehemann V, et al. Centrosomal aberrations in primary invasive breast cancer are associated with nodal status and hormone receptor expression. Int J Cancer 2003;107:346–52. [PubMed: 14506732]

44. Golubkov VS, Chekanov AV, Doxsey SJ, Strongin AY. Centrosomal pericentrin is a direct cleavage target of membrane type-1 matrix metalloproteinase in humans but not in mice: potential implications for tumorigenesis. J Biol Chem 2005;280:42237–41. [PubMed: 16251193]

45. Golubkov VS, Chekanov AV, Savinov AY, Rozanov DV, Golubkova NV, Strongin AY. Membrane type-1 matrix metalloproteinase confers aneuploidy and tumorigenicity on mammary epithelial cells. Cancer Res 2006;66:10460–5. [PubMed: 17079467]

46. Walter-Yohrling J, Morgenbesser S, Rouleau C, et al. Murine endothelial cell lines as models of tumor endothelial cells. Clin Cancer Res 2004;10:2179–89. [PubMed: 15041739]

47. Baeten CI, Wagstaff J, Verhoeven IC, Hillen HF, Griffioen AW. Flow cytometric quantification of tumour endothelial cells; an objective alternative for microvessel density assessment. Br J Cancer 2002;87:344–7. [PubMed: 12177806]

48. Vallentin A, Mochly-Rosen D. RBCK1, a protein kinase CbetaI (PKCbetaI)-interacting protein, regulates PKCbeta-dependent function. J Biol Chem 2007;282:1650–7. [PubMed: 17121852]

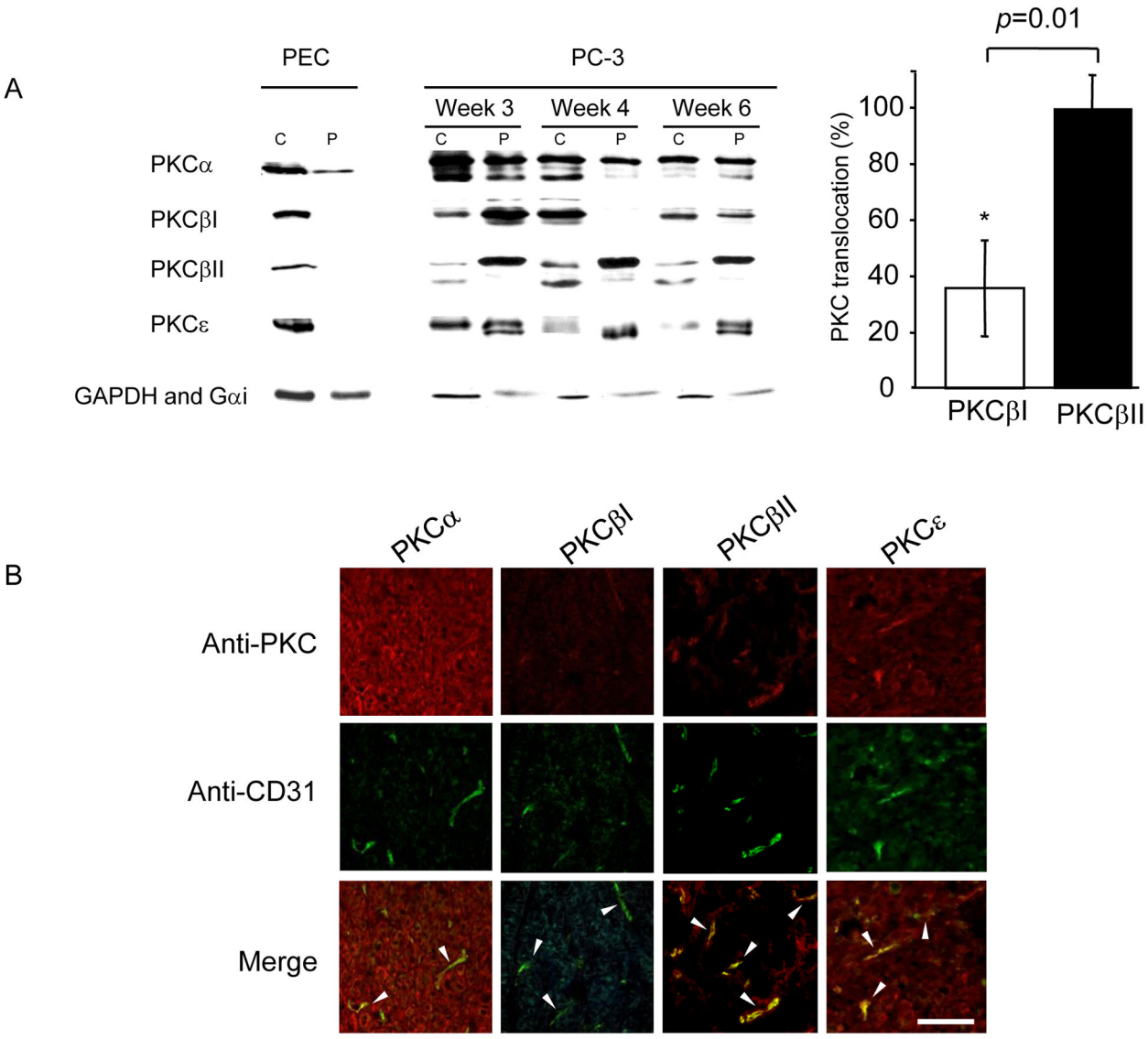

Figure 1.

PKCβII is active in growing PC-3 prostate tumors and is localized mainly in tumor endothelium as compared with other PKC isozymes. (A) The level of the active form of PKC isozymes was determined by Western blot analyses of cytosolic (C) and particulate (P) fractions from 3-, 4- and 6- week-old tumors using anti-PKCα, βI, βII and ε antibodies. Tumors were fractionated as described in Methods. Normal human prostatic epithelial cells (PEC) grown in serum-free medium (Complete PFMR-4A (24)) without bovine pituitary extract, were used to show basal levels of PKC translocation in this cell type. Quantification of the active forms of PKCβI and βII at week 6 (translocation; expressed as percentage of PKC isozyme in the particulate fraction over total cellular enzyme) is provided on the right (n=4, *; p=0.01). A 2-tailed Student's *t* test was used to determine significance. Loading controls for cytosolic and particulate fractions (GAPDH and Gαi) are shown. (B) Immunofluorescence staining of PC-3 prostate tumors 6 weeks after tumor implantation in mice demonstrated different levels of PKC isozymes in tumor vessels. Representative immunostaining using anti-PKCα, βI, βII, ε antibodies (red, top), anti-CD31 antibodies (green, middle) and merged images (yellow, bottom, arrow heads) are shown (n=5 each). Scale bar 10 μm.

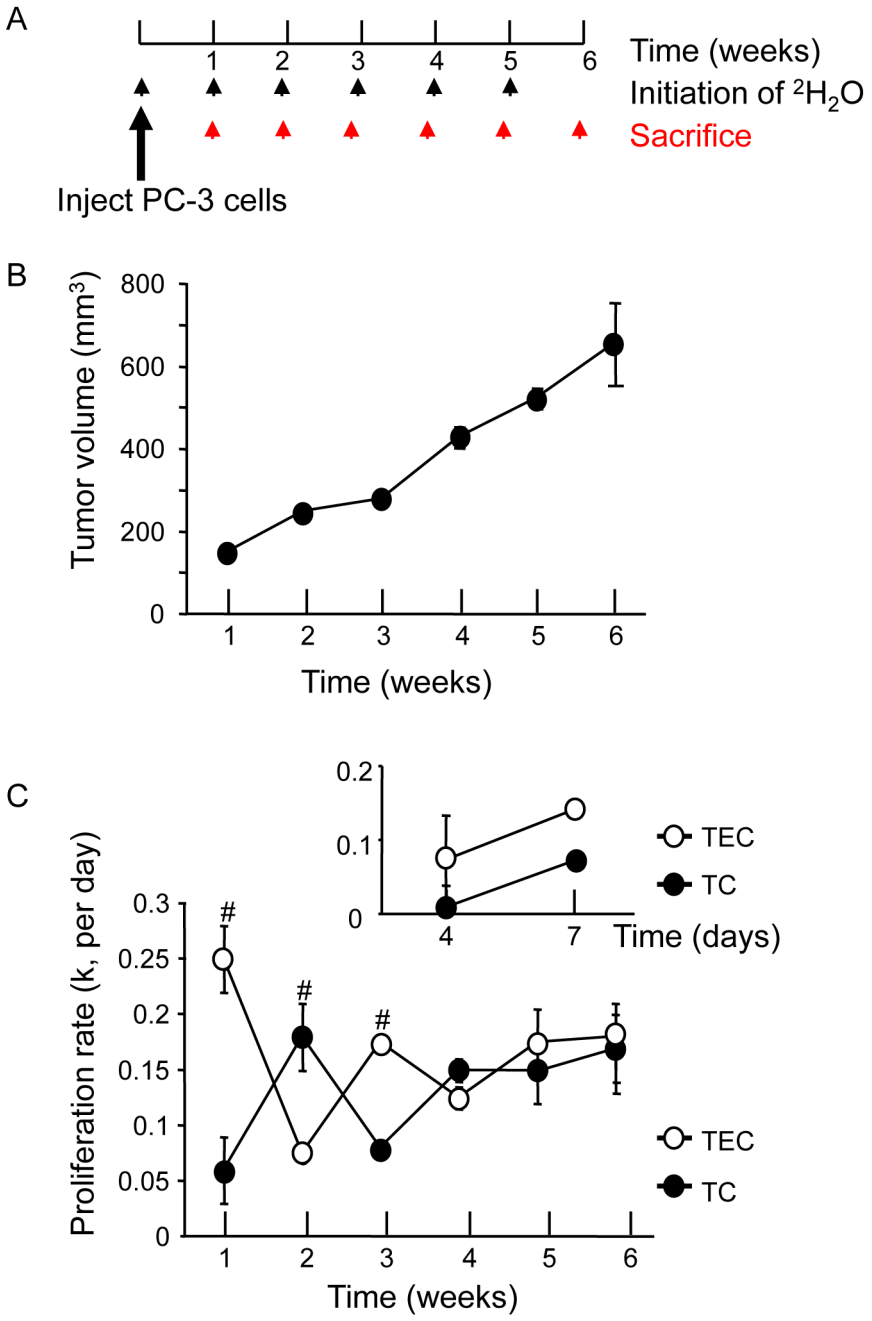

Figure 2.

In the early phase of tumor growth, an increase in endothelial cell proliferation rate precedes that of the tumor cells. (A) PC-3 tumor cells (5×10^6 cells) were injected *s.c.* into the left flank and the xenograft tumors were isolated each week up to 6 weeks after tumor implantation. Deuterated water was administered via *i.p.* injection (8%) and in the drinking water (4%) for 1 week prior to each study. (B) Tumor volume of PC-3 xenografts from week 1 to week 6 after tumor cell injection was measured using a caliper (mean±SEM). (C) Proliferation rates of isolated tumor endothelial cells (open circle) and tumor cells (filled circle) were analysed by GC-MS (n=4–7 per week). Different cell populations were isolated using FACS (see supplemental Figure 1). Proliferation rate [i.e. fractional turnover rate (k) per day] was

calculated as previously described (28, 29). Repeated ANOVA was used to determine the significance of differences between the curves. A 2-tailed Student's *t* test and ANOVA were used to determine the differences ($p<0.005$, repeated ANOVA; #; $p<0.05$, Student's *t* test). (Insert) The xenograft tumors were grown for 4 and 7 days after tumor cell injection and tumor endothelial cells and tumor cells were obtained to measure their proliferation rates. Deuterated water was administered for 4 days before sacrifice (n=6–10 per time point).

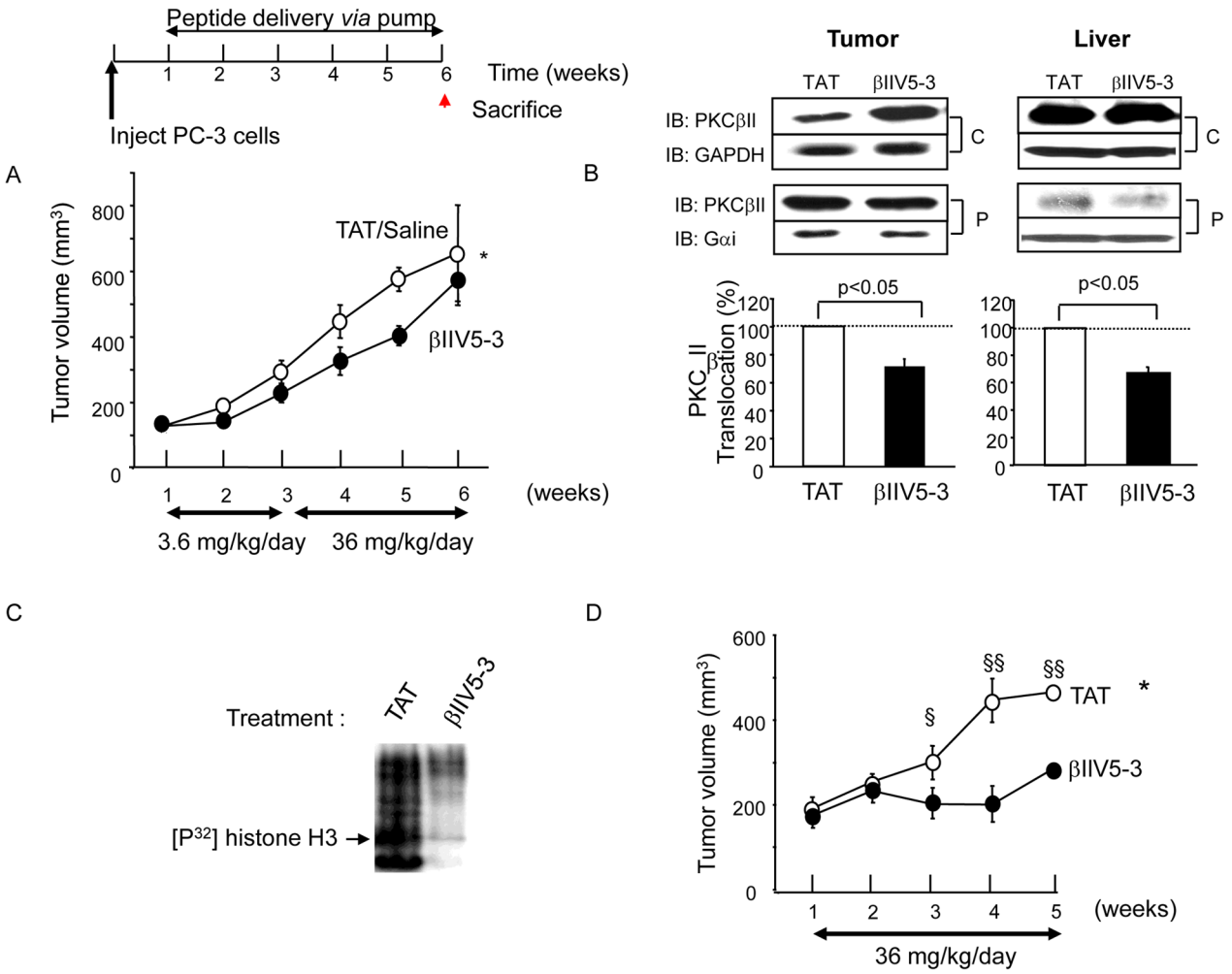

Figure 3.

PC-3 tumor growth rate was reduced with PKCβII-specific inhibitor treatment. One week after PC-3 cell injection, mice were implanted with osmotic pumps with saline, control peptide (TAT) or βIIV5-3 conjugated to TAT at 3.6 mg/kg/day for 2 weeks followed by 36 mg/kg/day for the next 3 weeks. Deuterated water (4%) was administered for 1 week prior to sacrifice. (A) Tumor volume was measured weekly (repeated ANOVA, *; $p<0.05$, n=4–5 each). Tumors were excised and weighed at week 6. Final tumor weight was 40% lower in the βII V5-3-treated group but this difference did not reach statistical significance and there was no difference in body weight between the groups. (B) Five-week continuous βIIV5-3-treatment decreased PKCβII translocation to the particulate fraction of both tumors and livers. The active level of PKCβII was analyzed by Western blot after fractionation. GAPDH and Gαi were used as loading controls for the cytosolic (C) and particulate (P) fractions, respectively. IB; immunoblot. A 2-tailed Student's *t* test was used to determine significance (n=3 each, $p<0.05$). (C) βIIV5-3 treatment *in vivo* results in reduced PKC kinase activity as measured *in vitro*, following immunoprecipitation with anti-PKCβII antibodies. Kinase assay was performed in the absence of added PKC activators, using histone (H3) as a substrate as described (30). The film was exposed for 3 days in −80C°. (D) A greater decrease in PC-3 tumor growth rate was obtained with a higher dose of βIIV5-3 (36 mg/kg/day for 4 weeks). A repeated ANOVA and a 2-tailed Student's *t* test was used to determine significance (*; $p<0.05$ in repeated ANOVA, §; $p<0.05$ *vs*. TAT-treated and §§; $p<0.005$ *vs*. TAT-treated in *t* test, n=8–9 each, 16% vs. 60%

reduction in the overall tumor growth rate, Figure 3A *vs.* 3D). Additional blots for (B) and (C) are provided in supplemental Figure 3.

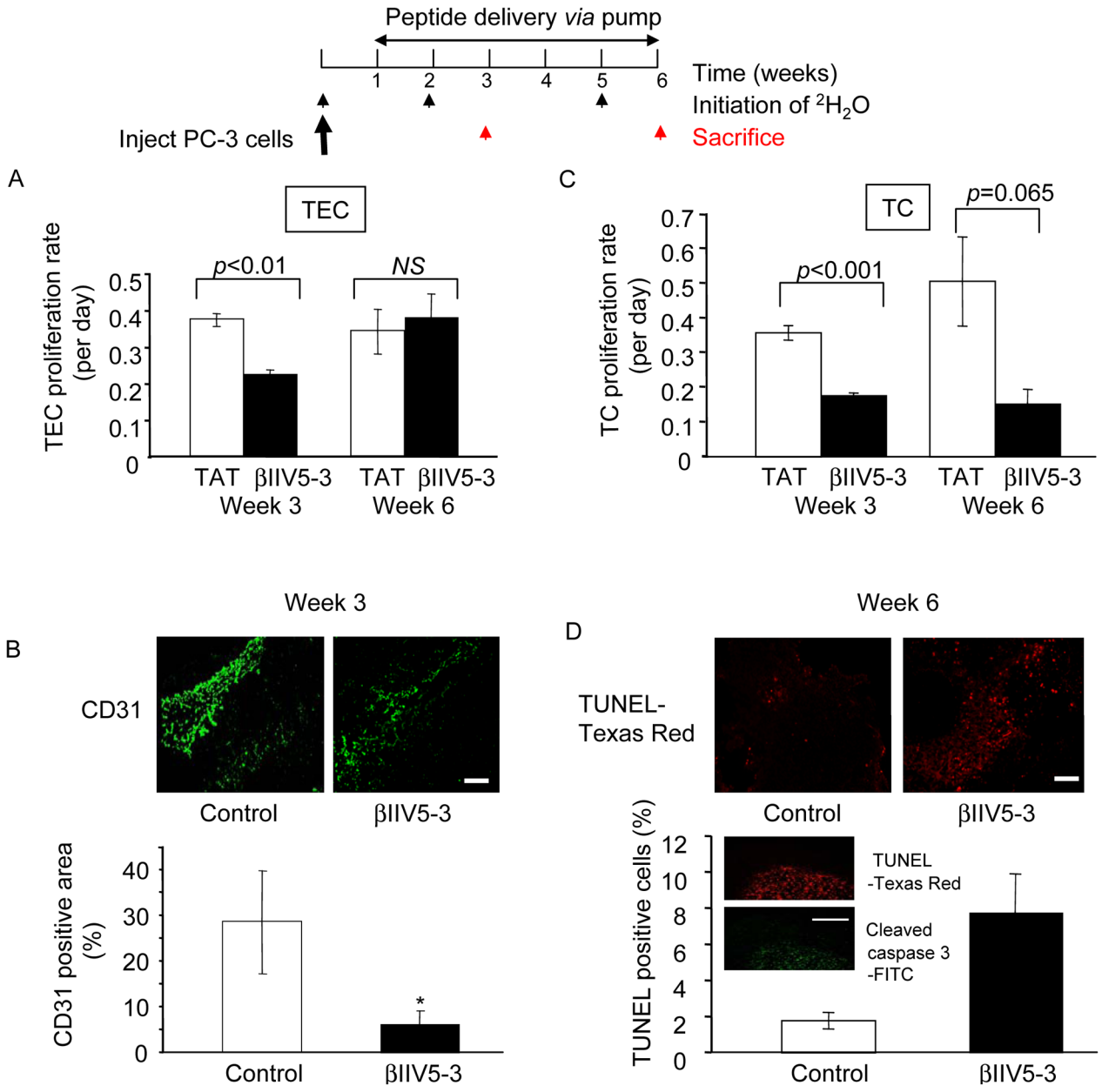

Figure 4.

Analysis of proliferation rates of tumor endothelial cells (TEC) and tumor cells (TC) after peptide treatment. (A) Mice treated with βIIV5-3 at 3.6 mg/kg/day for 2 weeks and with 36 mg/kg/day for the remaining 3 weeks were sacrificed at week 3 (mid point) and at the end of the treatment at week 6 and the proliferation rates of tumor endothelial cells were then determined after their isolation. Deuterated water was administered during the 7 days before sacrifice. A 2-tailed Student's *t* test was used to determine significance (Figure 4A, p=0.008 at week 3, n=8–9 each). (B). Tumor sections from week 3 and 6 were stained with CD31-FITC antibodies and immunostaining intensity was quantified using Photoshop. A 2-tailed Student's *t* test was used to determine significance (Figure 4B, week 3 data, *; p<0.05). Scale bar: 10 μm. (C) Mice treated with βIIV5-3 at 3.6 mg/kg/day for 2 weeks and with 36 mg/kg/day for the remaining 3 weeks were sacrificed at week 3 (mid point) and at the end of the treatment at

week 6 to isolate and determine proliferation rates of tumor cells. A 2-tailed Student's *t* test was used to determine significance (Figure 4C, p=0.0007 at week 3, n=8–9 each). (D) Tumor sections from week 3 and 6 were stained for TUNEL conjugated with Texas Red (Figure 4D, week 6 data, p=0.06, n=4). TUNEL staining was confirmed with cleaved caspase 3 staining (FITC- conjugated) of 3-week tumor samples (insert). Scale bars : 10 μm.

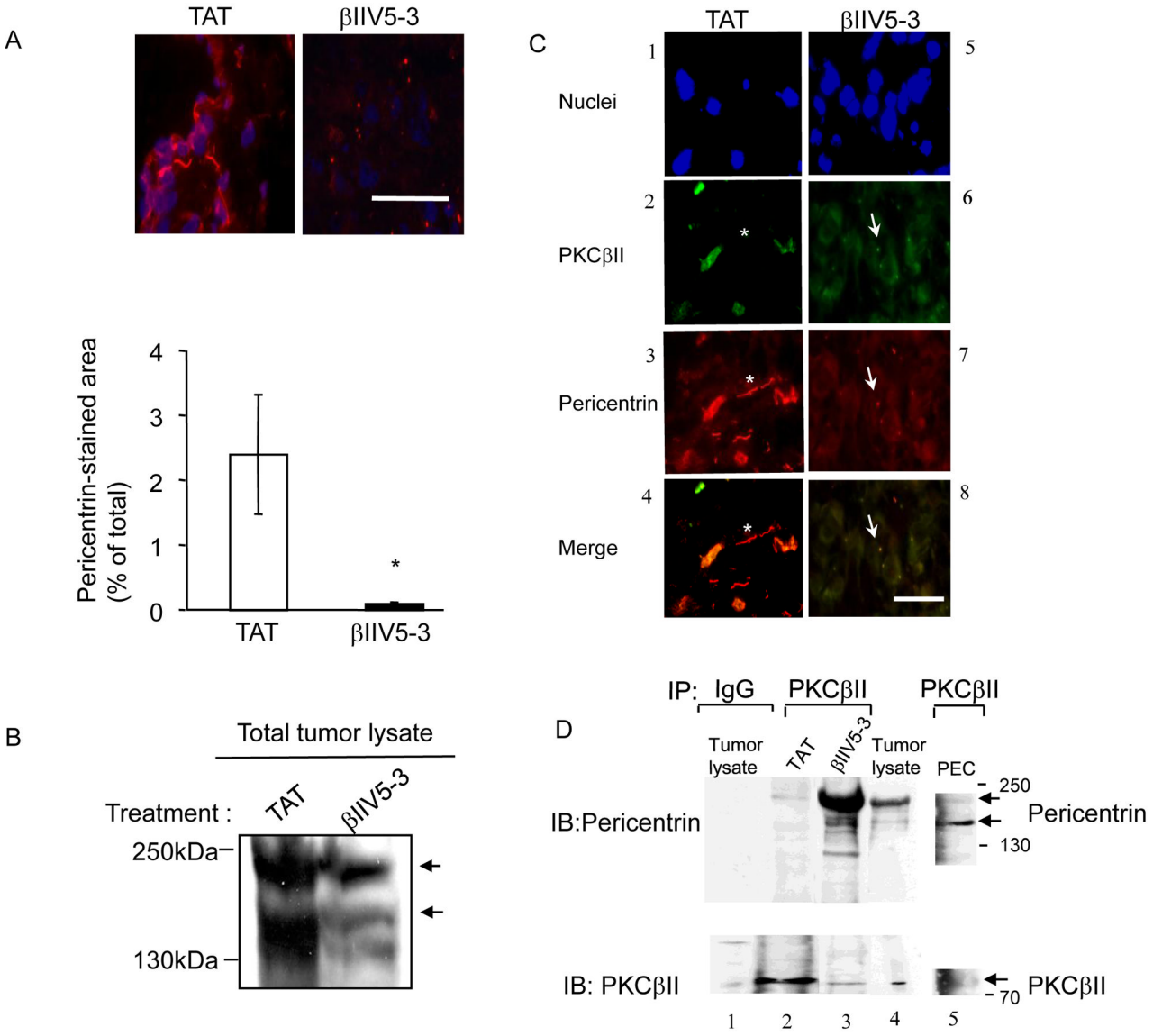

Figure 5.

βIIV5-3 treatment reduced pericentrin levels and induced co-localization of PKCβII and pericentrin in PC-3 tumors. (A) The level of pericentrin was determined using tumor sections after a 4-week treatment with TAT or βIIV5-3 at 36 mg/kg/day. Sections were stained for pericentrin (Abcam, rabbit polyclonal Ab4448; followed by goat anti-rabbit conjugated to Cy3, pink) and for nuclei (Hoechst, blue). (B) The levels of both the 220 and 150kDa bands corresponding to pericentrin (arrows, (22,44,45)) were determined using total tumor lysates after a 4-week treatment with TAT or βIIV5-3 at 36 mg/kg/day. (C) Immunofluorescence staining of 4-week-treated tumors demonstrated co-localization of PKCβII and normal dot-structured pericentrin in βIIV5-3-treated tumors. Shown are nuclei staining (panels B1 and 5), PKCβII (panels B2 and 6, green), pericentrin (panels B3 and 7, red) and merged figure (panels B4 and 8). Arrows indicate co-localization of pericentrin and PKCβII (yellow), whereas asterisk shows filamentous pericentrin not co-localized with PKCβII. (D) The interaction of PKCβII and pericentrin was further confirmed by immunoprecipitation (IP). Immunoprecipitates from the detergent- solubilized total tumor lysate and PEC cultures using anti-PKCβII antibody were immunoblotted (IB) with the mixture of 4b, M1 and UM225

pericentrin antibodies (19) to detect pericentrin (Figure 5C, top panel, lanes 2 and 3, arrows). Both the 220 and 150kDa bands corresponding to pericentrin (22,44,45) were present in immunoprecipitates showing that they interact with PKCβII *in vivo*. The interaction with PKCβII was stronger with βIIV5-3 treatment (compare top panel, lanes 2 and 3). In the negative control (lane 1, incubated with IgG and immunoprecipitated with beads), the amount of pericentrin (top panel, lane 1) or PKCβII (lower panel, lane 1) present was not significant. Whole tumor lysates of tumor was used as a positive control (lane 4) to show pericentrin and PKCβII bands (upper and lower panels, lane 4). Also, immunoprecipitate from the lysate of primary culture of PECs that were not treated with βIIV5-3 was used as another control to show interaction of PKCβII and pericentrin (Lane 5).

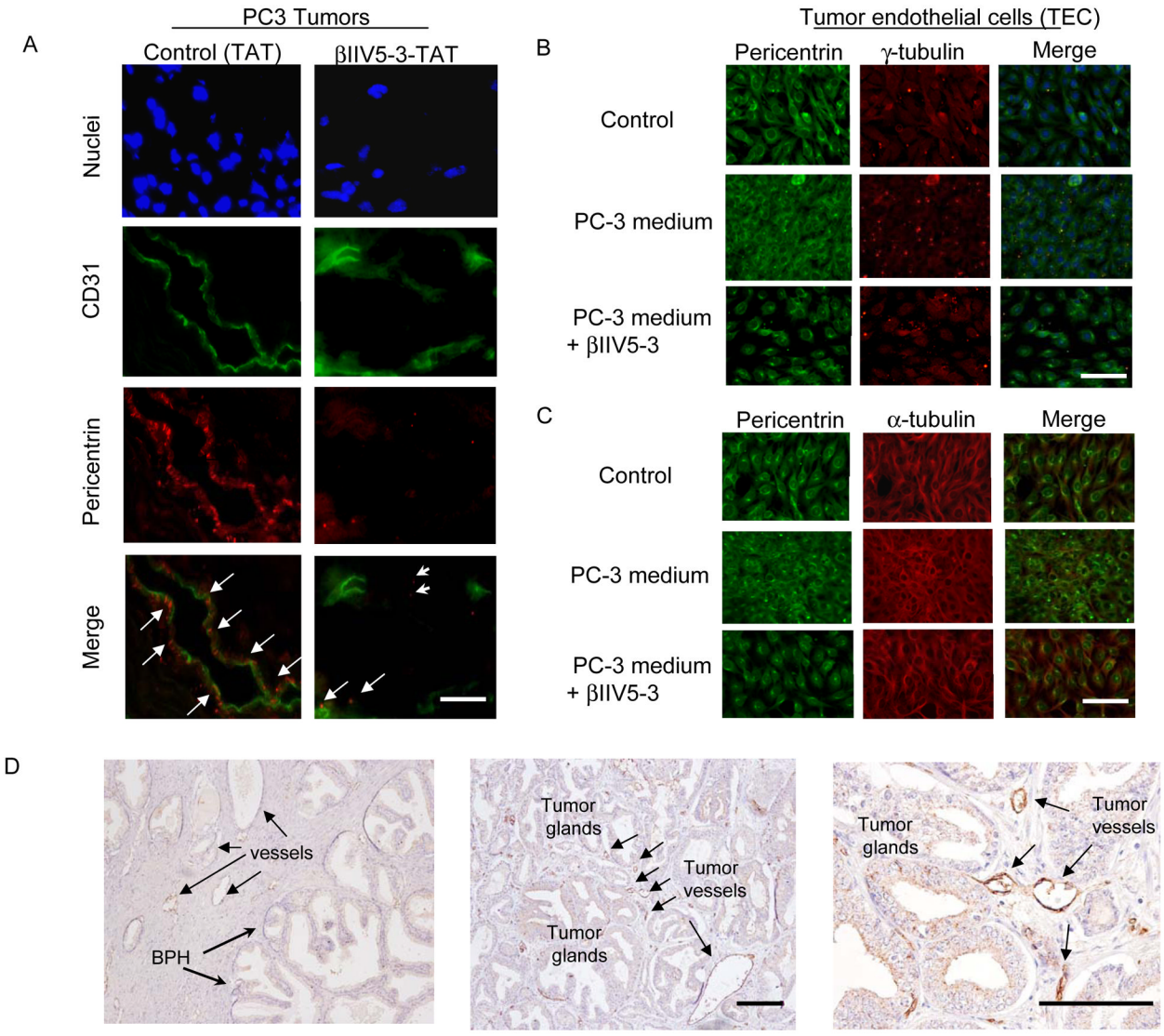

Figure 6.

Pericentrin abnormality is present in tumor endothelial cells and in human tumor endothelium. (A) Tumor sections from mice treated for 4 weeks with TAT or βIIV5-3 (36 mg/kg/day) were stained for nuclei (Hoechst), CD31 (green) and pericentrin (red). Scale bar: 10 μm. (B) The presence of abnormal pericentrin and centrosomal defects in tumor endothelial cells (TEC) grown in PC-3 conditioned medium was determined by immunofluorescence. Mouse tumor endothelial cells were grown in DMEM or in PC-3 conditioned medium (media from PC-3 cells grown for 2 days) and treated with TAT or βIIV5-3 at a final concentration of 1μM (added 3 times per day for 2 days). Representative images of TEC grown in DMEM with TAT (top), in PC-3 conditioned medium with TAT (middle) and with βIIV5-3 (bottom) are shown (representative of 3 experiments). Tumor endothelial cells were stained separately for pericentrin (green) and γ-tubulin (red). Merged figures are also shown (including nuclei stained with Hoechst). Scale bar: 10 μm. (C) Staining with anti-α-tubulin suggests abnormal microtubule structure in the tumor endothelial cells. Tumor endothelial cells treated the same as in (B) were stained separately for pericentrin (green) and α-tubulin (red). Merged figures are also shown (including nuclei staining with Hoechst). Scale bar: 10 μm. (D) The level of pericentrin is high in human prostate tumor endothelium. The level of pericentrin was

determined using paraffin-embedded sections from human prostate with Gleason grades 3, 4 and 5 cancers and were stained for pericentrin and counterstained with hematoxylin. Representative pictures are shown (n=8; left: pericentrin staining on endothelium adjacent to benign prostatic hyperplasia, middle: pericentrin staining on tumor endothelium adjacent to tumor glands with Gleason grades 3+4, right: magnified view of the middle figure). Scale bars: 10 μm.